

## The Magnetic Structures of the Layer Ferri-magnets $P(C_6D_5)_4M^{II}Fe(C_2O_4)_3$ ( $M^{II} = Mn, Fe$ )

Christopher J. Nuttall and Peter Day\*

Davy Faraday Research Laboratory, The Royal Institution of Great Britain, 21 Albemarle Street, London W1X 4BS

Received February 24, 1998

The bimetallic trisoxalatometal(II,III) salts with the general formula  $AMM'(C_2O_4)_3$ , first reported by Tamaki et al.,<sup>1</sup> form a fascinating series in which to establish structure–property relationships in two-dimensional molecular-based lattices. The organic cation A can be varied widely, so that interlayer separations range from 8.5 to 14.5 Å;<sup>2</sup> the transition metal ions M and M' are also capable of wide variation, leading to ferro- or antiferromagnetic near-neighbor exchange and either ferro- or ferrimagnetic bulk properties. The oxalate ions bridge M and M', which, having 6-fold coordination, therefore form honeycomb layers.<sup>3–5</sup> Within this broad series the compounds having M' = Fe(III) are especially interesting from a magnetic point of view. When M = Mn(II) we have the rare situation of a bimetallic lattice in which both metal ions have the same electronic ground state,  $3d^5$ ,  $S = 5/2$ ,  $^6A_1$ . In case of antiferromagnetic near-neighbor exchange, the bulk properties should mimic those of an antiferromagnet rather than a ferrimagnet, since the two ions only differ marginally in their  $g$  values. This is indeed so,<sup>2</sup> though the magnitude of the uncompensated moment, while small, is extremely sensitive to the organic counteranion A. When M = Fe(II) an even more fascinating situation arises: not only are the compounds mixed valency (albeit of class II,<sup>6</sup> i.e., valence-trapped, type) but since the Fe(II) ion has a large anisotropy the bulk magnetic behavior is highly unusual, with strong negative magnetization at low fields for some A.<sup>2,7</sup> Definitive evidence on the ordered magnetic structures of solids comes from neutron diffraction. To date the only published work on the magnetic structure of a layer bimetallic trisoxalate salt using this method refers to a  $Mn^{II}-Cr^{III}$  phase which is ferromagnetic.<sup>8</sup> In the present note we report a neutron powder diffraction study of the two antiferromagnetic phases  $P(C_6D_5)_4M^{II}Fe(C_2O_4)_3$  with  $M^{II} = Mn$  and Fe.

### Experimental Section

Neutron powder diffraction data were collected using three instruments at the Institut Laue-Langevin, Grenoble, France. The D1B diffractometer is a high-intensity, medium-resolution, multidetector diffractometer. The wavelength is fixed at 2.52 Å, by a graphite

focusing monochromator. Counts are collected in steps of 0.2°, as defined by the distance between adjacent detector cells in the PSD bank. D1A has a high takeoff angle of 122° giving a good resolution over  $2\theta = 6–160^\circ$ . Scans are taken in 0.05° steps. The wavelength employed was 2.9811 Å, Ge[113]. A graphitic filter between the monochromator and the sample significantly reduced higher-order wavelength contaminations ( $\lambda/3 < 0.1\%$ ). D2B is a very high resolution constant-wavelength diffractometer. Data collection is by step scans of 0.05°. A graphitic filter similar to that of D1A allowed collection at the relatively high wavelength of 2.398 Å (Ge[331]) without significant contamination from higher-order wavelengths. The instrument was set in its high-intensity mode.

The deuterated tetraphenylphosphonium cation  $P(C_6D_5)_4^+$  was prepared as its bromide salt by a method modified from that originally proposed by Michealis<sup>9</sup> and Dodanov<sup>10,11</sup> for the synthesis of  $P(C_6H_5)_4Br$ . Bromobenzene(-*d*<sub>5</sub>) and triphenylphosphine(-*d*<sub>15</sub>) were used as purchased from Aldrich Chemicals Ltd. (deuteration >99.8%). The prepared  $P(C_6D_5)_4Br$  was confirmed to be >99% deuterated by mass spectrometry (performed by John Hill at UCL).

$P(C_6D_5)_4MnFe(C_2O_4)_3$  and  $P(C_6D_5)_4FeFe(C_2O_4)_3$  were prepared as follows.

**$P(C_6D_5)_4MnFe(C_2O_4)_3$ .** A solution containing 3.344 g of  $Fe(NO_3)_3 \cdot 6H_2O$  (9.56 mmol) and 1.885 g of  $MnCl_2 \cdot 6H_2O$  (9.56 mmol) in 64 mL of  $H_2O$  was prepared; 3.671 g of  $H_2C_2O_4 \cdot 2H_2O$  was dissolved in it. After 1 h the solution was filtered, and 2.65 g of  $P(C_6D_5)_4Br$  (6.38 mmol), dissolved in 11 mL of 70:30 MeOH/ $H_2O$ , was added dropwise to the filtrate. The precipitated  $P(C_6D_5)_4MnFe(C_2O_4)_3$  was removed by filtration and dried {yield = 3.55 g (80%)}.

**$P(C_6D_5)_4FeFe(C_2O_4)_3$ .** A solution containing 2.271 g of  $Fe(NO_3)_3 \cdot 6H_2O$  (6.5 mmol) and 1.804 g of  $FeSO_4 \cdot 6H_2O$  (6.5 mmol) in 50 mL of  $H_2O$  was prepared; 2.496 g of  $H_2C_2O_4 \cdot 2H_2O$  was dissolved in it. After 1 h the solution was filtered, and 1.9 g of  $P(C_6D_5)_4Br$  (4.329 mmol), dissolved in 11 mL of 70:30 MeOH/ $H_2O$ , was added dropwise to the filtrate. The precipitated  $P(C_6D_5)_4FeFe(C_2O_4)_3$  was removed by filtration and dried {yield = 2.05 g (71.7%)}.

X-ray diffraction profiles of the two compounds verified that they were free of  $M^{II}C_2O_4 \cdot 2H_2O$  peaks.

### Results

The neutron powder diffraction profile of the MnFe compound recorded on D1A at 40 K is displayed in Figure 1a, and that of the FeFe compound, recorded at 50 K on D2B, is in Figure 1b. Using profile matching,<sup>12</sup> i.e., iterative fitting of structure factors, both were fitted with a Gaussian peak shape and  $R3c$  unit cell  $\{\chi^2(MnFe) = 0.53, \chi^2(FeFe) = 0.47\}$ . The fit gave lattice parameters of  $a, b = 18.831(4)$  and  $18.674(8)$  Å and  $c = 55.511(8)$  and  $56.289(14)$  Å, respectively, which correspond well with those obtained by room-temperature X-ray diffraction,<sup>2,8</sup> with the expected contraction in  $c$  ( $\sim 2$  Å) and  $a, b$  ( $\sim 0.5$  Å) on decreasing the temperature. The intensity not fitted by the profile matching procedure is attributed to a small fraction of  $P6(3)$  stacking phase identified in X-ray diffraction profiles. The 1.5 K profiles revealed no significant change in lattice parameters between 1.5 and 40 K. However, in the MnFe compound a number of reflections had increased intensity in the 1.5 K profile due to magnetic diffraction arising from long-range magnetic order. In contrast, in the FeFe compound, the only extra intensity at 1.5 K was a weak shoulder to the [202] nuclear reflection.

- (1) Tamaki, H.; Zhong, Z. J.; Matsumoto, N.; Kida, S.; Koikawa, M.; Achiwa, N.; Hashimoto, Y.; Okawa, H. *J. Am. Chem. Soc.* **1992**, *114*, 6974.
- (2) Mathonière, C.; Nuttall, C. J.; Carling, S. G.; Day, P. *Inorg. Chem.* **1996**, *35*, 1201.
- (3) Decurtins, S.; Schmalle, H. W.; Oswald, H. R.; Linden, A.; Ensling, J.; Gütlich, P.; Hauser, A. *Inorg. Chim. Acta* **1994**, *216*, 65.
- (4) Atovmyan, L. O.; Shilov, G. V.; Lyobovskaya, R. N.; Zhilyaeva, E.; Ovanesyan, N. S.; Pirumova, S. A.; Gusakovskaya, I. G. *JETP Lett.* **1993**, *58*, 766.
- (5) Carling, S. G.; Mathonière, C.; Day, P.; Malik, K. M.; Coles, S. J.; Hursthouse, M. B. *J. Chem. Soc., Dalton Trans.* **1996**, 1839.
- (6) Robin, M. B.; Day, P. *Adv. Inorg. Chem. Radiochem.* **1966**, *10*, 247.
- (7) Mathonière, C.; Carling, S. G.; Yusheng, D.; Day, P. *J. Chem. Soc., Chem. Commun.* **1994**, 1551.
- (8) Pellaux, R.; Schmalle, H. W.; Huber, R.; Fischer, P.; Hauss, T.; Ouladdiaf, B.; Decurtins, S. *Inorg. Chem.* **1997**, *36*, 2301.

- (9) Michealis, D.; Soden, V. *Annales* **1885**, 229, 298.
- (10) Dodanov, R.; Medox, S. *Ber.* **1928**, *61*, 907.
- (11) Nuttall, C. J. Thesis, University of London, 1998.
- (12) Rodriguez-Carvajal, J. *FULLPROF: Reference Guide to the Program 3.2*; CEA-CNRS: Paris, 1997.

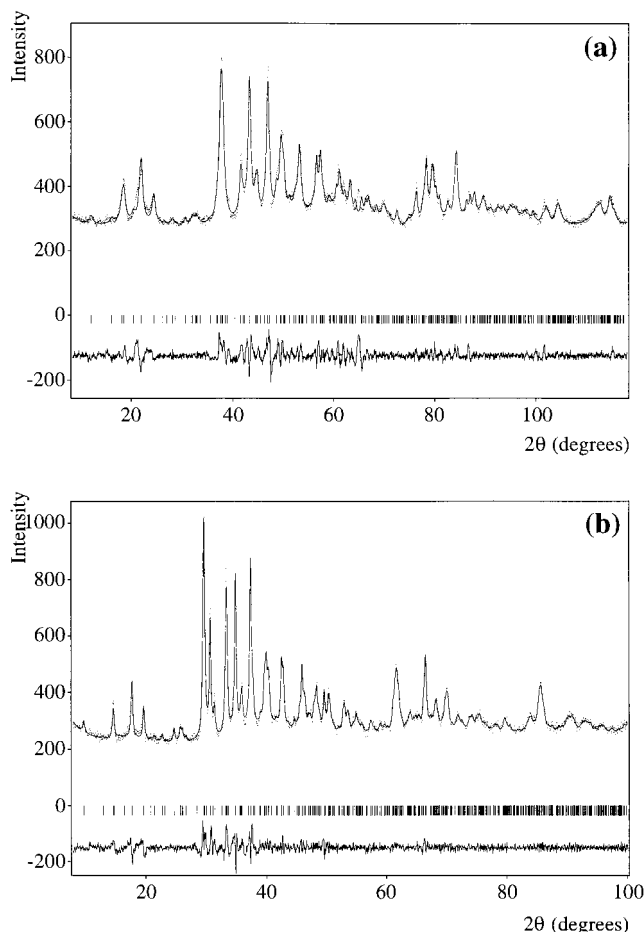


**Figure 1.** Neutron diffraction profiles of  $P(C_6D_5)_4M^{II}Fe(C_2O_4)_3$  fitted with pattern matching to an  $R3c$  cell: (a)  $M^{II} = Mn$ , 40 K (D1A) ( $10 < 2\theta < 120^\circ$ ); (b)  $M^{II} = Fe$ , 50 K (D2B) ( $10 < 2\theta < 120^\circ$ ).

The magnetic diffraction intensity was investigated in greater detail by means of difference plots obtained with the higher-flux D1B diffractometer. The intensity difference ( $[I(1.7\text{ K}) - I(T > T_c)]$ ) is plotted in Figure 2. The magnetic reflections are quite weak compared to the large fluctuations in the difference background; however, the magnetic intensity can be indexed using an  $R3c$  cell. The most intense magnetic reflection [201] observed in the difference plots was integrated, and its temperature dependence is plotted in Figure 3. The sharp decrease of the magnetic intensity at 24 and 39 K for the MnFe and FeFe compounds, respectively, compares well with the ordering temperatures estimated by bulk susceptibility measurements. While the temperature dependence of the FeFe magnetic intensity approximates a Brillouin function, that of MnFe is more complex and probably contains a contribution from short-range order above  $T_c$  which cannot be deconvoluted from powder data.

The indices of the magnetic reflections of MnFe (Figure 2a) indicate that the chemical and magnetic cells are coincident, i.e., the magnetic structure has the propagation vector  $\kappa = 0$ , and also that the moments lie close to the  $c$  axis, since no intensity is found for [00 $l$ ] reflections. In the  $R3c$  cell both antiferromagnetic and ferromagnetic magnetic ordering models with  $\kappa = 0$  can be envisaged with moments aligned parallel to the  $c$  axis. However, ferromagnetic ordering can be discounted as susceptibility measurements indicate antiferromagnetic ordering in the hydrogenous compound  $P(C_6H_5)_4MnFe(C_2O_4)_3$ .<sup>2</sup> Possible antiferromagnetic ordering models with moments parallel to the  $c$  axis may be further defined by considering the character of axial spins with respect to the symmetry operations

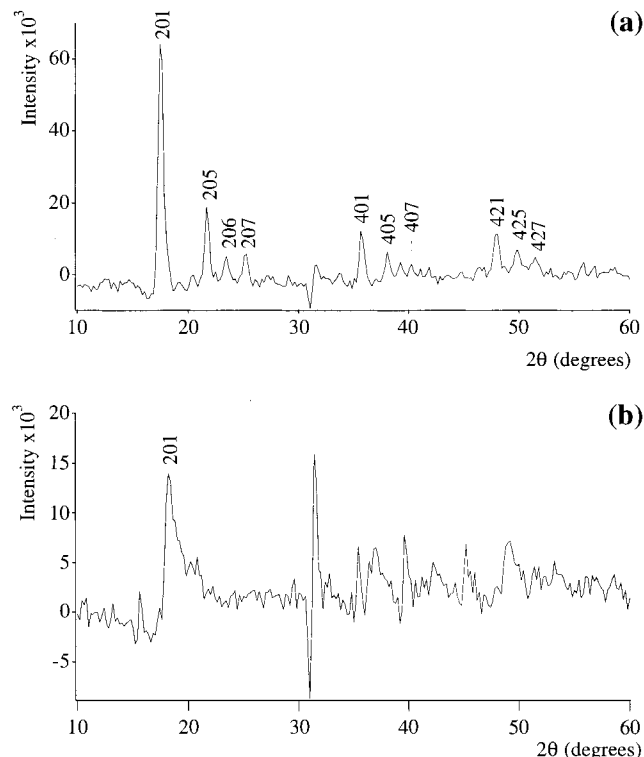


**Figure 2.** Intensity difference  $[I(1.7\text{ K}) - I(T > T_c)]$  for  $P(C_6D_5)_4M^{II}Fe(C_2O_4)_3$  with magnetic reflections ( $R3c$  cell) indicated: (a)  $M^{II} = Mn$ ,  $T = 30\text{ K}$ ; (b)  $M^{II} = Fe$ ,  $T = 50\text{ K}$ .

of the group. Two models are generated by considering the moment characters associated with the  $c$  glide plane operation in  $R3c$ , namely, antiferromagnetism with and without inversion of axial components of the moment along the  $c$  glide plane; respectively these are  $R3c$  and  $R3c'$  according to the Shubnikov definition. They differ in that  $R3c$  requires the orientations of Mn and Fe moments to alternate from up to down in adjacent layers while in  $R3c'$  they have the same relative orientation in all layers.

Using the FULLPROF program,<sup>12</sup> profiles were generated for the antiferromagnetic models  $R3c$  and  $R3c'$  using the metal positions<sup>3</sup> from the structure of  $P(C_6H_5)_4MnCr(C_2O_4)_3$  and the fitted low-temperature cell constants from the neutron data. For each model a moment of  $5\ \mu_B$  was placed antiparallel along the  $c$  axis on the  $Mn^{2+}(\uparrow)$  and  $Fe^{3+}(\downarrow)$  sites. The predicted profiles are plotted in Figure 4.

By comparing the observed and predicted patterns, it is clear that the  $R3c$  Shubnikov group provides the best representation of the low-temperature magnetic order in the MnFe compound. The proposed magnetic structure is illustrated in Figure 5. There are a few reflections in the magnetic profile which are not predicted by this model, the most prominent being [206]. The extra magnetic intensity could result from either the presence of a small amount of a  $P6(3)$  stacking phase previously identified or from magnetic order in  $R3c$  with moments not exactly aligned along the  $c$  axis. The first alternative was investigated by constructing a cell in  $P6(3)$  using the metal atom positions from the  $P6(3)$  half-cell structure of  $N(C_4H_9)_4MnFe(C_2O_4)_3$ .<sup>8</sup> Calculated profiles for this structure, with antiferromagnetic alignment along the  $c$  axis for either  $P6(3)$  or  $P6(3)'$  stacking, predict a high intensity for the [102(206)] reflection, but [100(200)] is predicted to have even higher intensity although it is not observed. Hence the first alternative can be discounted, i.e., labeling reflections in both  $P6(3)$  and the  $R3c$  super cell as  $[P6(3)(R3c)]$ .

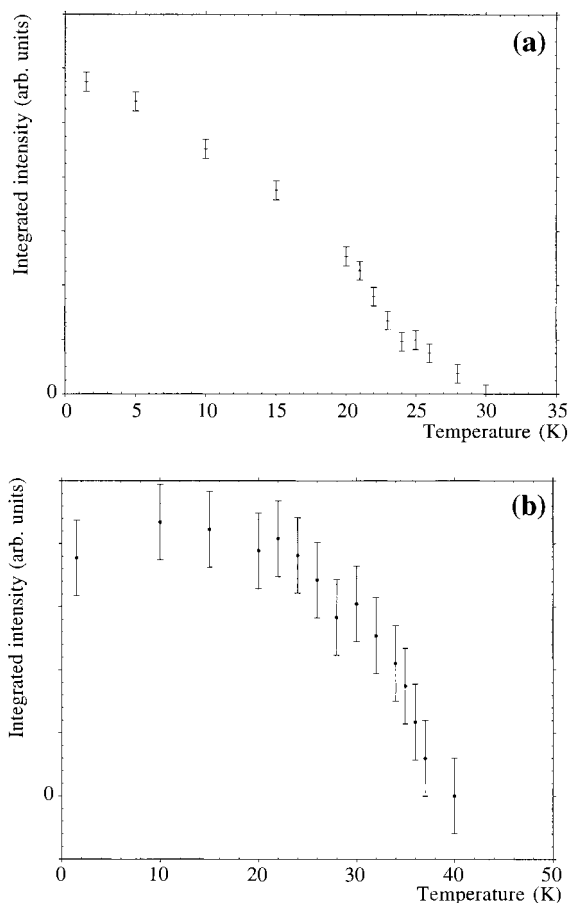


**Figure 3.** Integrated intensity of the [201] magnetic reflection of  $P(C_6D_5)_4M^{II}Fe(C_2O_4)_3$  versus temperature: (a)  $M^{II} = Mn$ ; (b)  $M^{II} = Fe$ .

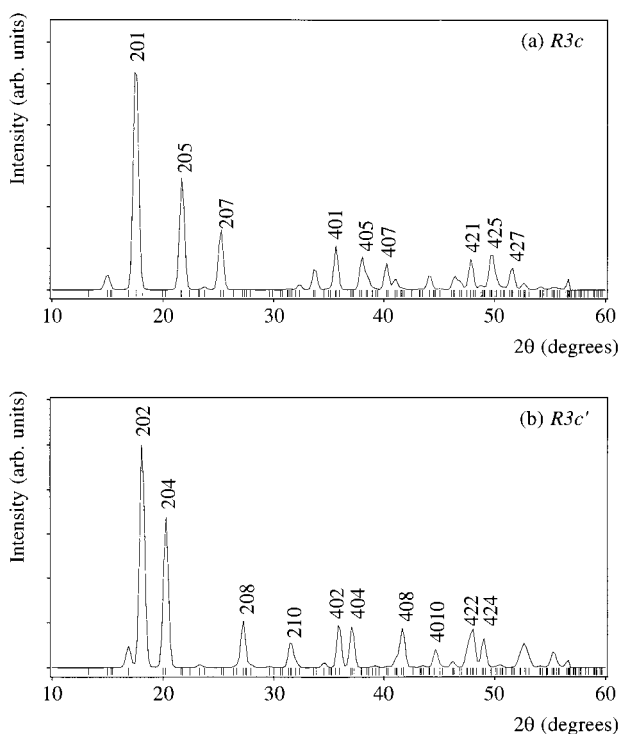


**Figure 4.** Predicted magnetic diffraction patterns for antiferromagnetic alignment along the  $c$  axis in  $P(C_6D_5)_4M^{II}Fe(C_2O_4)_3$ : (a)  $R3c$ ; (b)  $R3c'$ .

The alternative of antiparallel antiferromagnetic ordering with moments oriented away from the  $c$  axis was investigated by

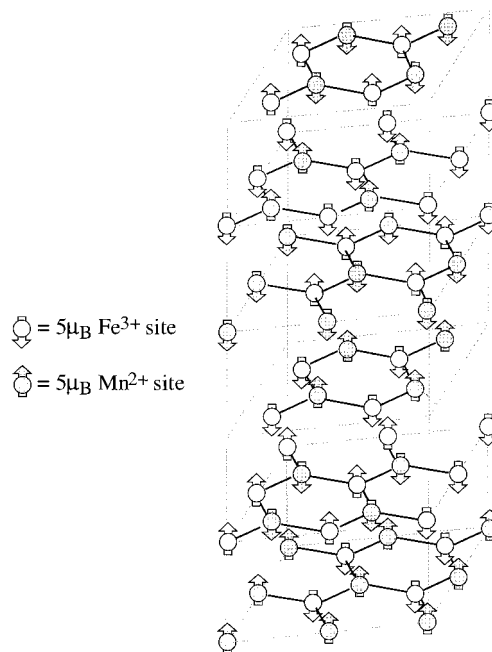


**Figure 5.** Proposed magnetic structure of  $P(C_6D_5)_4MnFe(C_2O_4)_3$ .

generating magnetic profiles with moments on  $Mn(\uparrow)$  and  $Fe(\downarrow)$  inclined at various angles to the  $c$  axis (using the  $R3c$  Shubnikov group), with nonaxial moment components parallel to the  $a$  axis. Altering the nonaxial spin direction between the  $a$  and  $b$  axes caused little change in the predicted pattern because of the almost exact hexagonal arrangement of the metal atoms in the  $(a,b)$  plane. The intensity of the [206] magnetic reflection does not increase significantly, while those of [006] and [204], which we do not observe, increase greatly. Thus there is no evidence that the moments are aligned other than parallel to the  $c$  axis.

In striking contrast to the  $MnFe$  compound, the intensity difference plot [ $I(1.7\text{ K}) - I(50\text{ K})$ ] of the  $FeFe$  compound (Figure 2b) reveals only extremely weak magnetic scattering. That the single clearly observed peak indexes as [201] indicates antiferromagnetic order of the  $Fe(II)$  and  $Fe(III)$  moments parallel to the  $c$  axis. However, the [201] reflection is highly asymmetric, which strongly suggests that there is disorder between the layers. Nevertheless, the bulk susceptibility measurements suggested a transition to long-range order at 34 K.<sup>2</sup> In view of these facts, one possible view of the magnetic order is that the behavior is glassy as a result of the strong single-ion anisotropy of the  $Fe(II)$  ions: below 39 K ferrimagnetic correlations develop with anisotropy directions randomly oriented in different layers. Finally the correlated regions become blocked by each other so that, while the majority of the moments are fixed by anisotropy pinning, a fraction remains mobile down to 5 K.

## Conclusion

Neutron powder diffraction reveals contrasting low-temperature magnetic order in the bimetallic layer ferrimagnets  $P(C_6D_5)_4M^{II}Fe(C_2O_4)_3$  ( $M^{II} = Mn, Fe$ ). In the  $MnFe$  compound the observed magnetic diffraction agrees very well with that predicted for a simple collinear antiferromagnetic alignment of  $Mn(II)$  and  $Fe(III)$  moments parallel to the  $c$  axis (i.e. perpendicular to the layers) with Shubnikov  $R3c$  symmetry. This model correctly describes the relative intensities of the four most intense magnetic reflections, and also the presence of weaker

observed peaks predicted by the model. In contrast, in the FeFe compound the magnetic diffraction is much weaker and only a single reflection [201] is observed. Absence of [00 $l$ ] intensity indicates that, like the MnFe compound, the moments in FeFe are aligned antiferromagnetically along or close to the  $c$  axis. However, the asymmetric line shape of the [201] reflection suggests that full long-range order is not fully established, even

at 5 K, possibly because randomly oriented domains with differing anisotropy directions develop and become blocked.

This work has been supported by the UK Engineering and Physical Sciences Research Council (studentship to C.J.N.). We are grateful to the Institut Laue-Langevin, Grenoble, for access to neutron facilities and to Dr A. Hewat for help and discussions.

IC980201S